



PII S0016-7037(97)00364-5

## Kinetics and mechanisms of precipitation of calcite as affected by $P_{\text{CO}_2}$ and organic ligands at 25°C

I. LEBRÓN\* and D. L. SUÁREZ

U.S. Salinity Laboratory, Riverside, California 92507, USA

(Received March 12, 1997; Accepted in revised form October 2, 1997)

**Abstract**—This study was conducted to develop a model for the precipitation rate of calcite under varying  $\text{CO}_2$  partial pressures and concentrations of dissolved organic carbon (DOC). Precipitation rates of calcite were measured in solutions with supersaturation values ( $\Omega$ ) between 1 and 20 and in the presence of  $2 \text{ m}^2 \text{ L}^{-1}$  of calcite. Experiments were run at partial pressures of  $\text{CO}_2$  ( $P_{\text{CO}_2}$ ) in the range of 0.035–10 kPa and DOC concentrations in the range of 0.02–3.50 mM. The effects of these two variables were quantified separately for the precipitation mechanisms of crystal growth and heterogeneous nucleation. We found an increase in precipitation rate (at constant  $\Omega$ ) when  $P_{\text{CO}_2}$  increased. For constant  $\Omega$ , we also found a linear relationship between calcite precipitation rate and activity of  $\text{CaHCO}_3^+$ , indicating that  $\text{CaHCO}_3^+$  species have an active role in the mechanism of calcite precipitation. These findings suggest that the increase in the precipitation rate with higher  $P_{\text{CO}_2}$  levels is likely caused by the increase in the negative charge on the calcite surface together with an increase in the activity of  $\text{CaHCO}_3^+$  species in solution. The mechanism of inhibition of calcite crystal growth by organic ligands has been shown to be surface coating of the crystals by DOC. The amount of DOC adsorbed on the surface of the calcite crystals follows a Langmuir isotherm for all the  $P_{\text{CO}_2}$  levels studied; however, the amount of DOC necessary to inhibit calcite precipitation increased. With increasing  $P_{\text{CO}_2}$ , the negative charge on the crystal increases, which affects crystal growth, but also these increases in  $P_{\text{CO}_2}$  cause a decrease in the solution pH and increase in the ionic strength for constant  $\Omega$ . Solution pH and ionic strength affect the structure and degree of dissociation of the organic functional groups, which in turn affects the inhibition of crystal growth and heterogeneous nucleation. The effect of  $P_{\text{CO}_2}$  and DOC concentration on the precipitation rate of calcite is expressed in a precipitation rate model which reflects the contributions of crystal growth and heterogeneous nucleation. Copyright © 1998 Elsevier Science Ltd

### 1. INTRODUCTION

Carbonate minerals are ubiquitous and play an important role in the geochemistry of natural environments. Precipitation and dissolution of carbonates affect most of the biogeochemical processes of aquatic systems and can influence the cycling of major and trace elements. There is extensive evidence that calcite precipitation in natural environments is a kinetically controlled process, but very few precipitation studies have been conducted under circumstances that simulate natural conditions.

The literature on the solution kinetics of calcite in clean systems is extensive (Nancollas and Reddy, 1971; Reddy and Nancollas, 1973; Plummer et al., 1978; Morse, 1983; Mucci and Morse, 1983; Buhmann and Dreybrodt, 1985 a, b; Inskeep and Bloom, 1985, 1986; Busenberg and Plummer, 1986; Mucci, 1986; Compton et al., 1989; Compton and Unwin, 1990; Compton and Pritchard, 1990; and Brown et al., 1993). In these studies the effects of pH and  $P_{\text{CO}_2}$  on calcite dissolution and precipitation are quantified for temperatures from 5 to 60°C. Shiraki and Brantley (1995) presented a kinetic model for calcite precipitation at near-equilibrium conditions at 100°C. In their model, based on Nielsen (1983), Shiraki and Brantley (1995) include three reaction mechanisms for calcite precipitation and define the conditions of the system at which each one of the mechanisms occur. Although developed for high temperatures, the Shiraki and Brantley (1995) model pre-

sents a basis for a better understanding of calcite crystal growth at 25°C. They maintain that spiral growth, adsorption, and surface nucleation occur during calcite precipitation, and the importance of the different mechanisms depends on the initial conditions of the system. Different stages of calcite precipitation were initially proposed by Nancollas and Reddy (1971) and have been observed by Dove and Hochella (1993) using atomic force microscopy.

Water soluble organic ligands and ions such as  $\text{PO}_4^{3-}$  have been known to act as precipitation inhibitors by blocking crystal growth sites (Kitano and Hood, 1965; Reddy, 1977; Reynolds, 1978; Reddy and Wang, 1980; Inskeep and Bloom, 1986; Dove and Hochella, 1993; Gratz and Hillner, 1993; Katz et al., 1993; Paquette et al., 1996). In a seeded crystal growth experiment Inskeep and Bloom (1986) found that the precipitation rate constant decreased to zero at  $\Omega = 8-9$  ( $\Omega = \text{IAP}/K_{\text{SP}}$ , where IAP is the ionic activity product, and  $K_{\text{SP}}$  is the solubility product of pure calcite at 25°C) in the presence of 0.15 mM dissolved organic carbon (DOC) from a water-soil extract. Levels of DOC in natural environments are comparable to the levels found by Inskeep and Bloom (1986) to inhibit calcite precipitation; however, most calcite precipitation models do not account for organic matter inhibition. The only currently available model that predicts the calcite precipitation rate in the presence of DOC is the model by Lebron and Suarez (1996). They found that when the DOC  $\geq 0.05$  mM, the precipitation rate is essentially independent of the surface area of the calcite and dependent on the DOC concentration.

The Lebron and Suarez (1996) model was developed for

\* Author to whom correspondence should be addressed (ilebron@ussl.ars.usda.gov).

Table 1. Synthesis of the experiments performed

Objective	Total Number of Experiments	Repetitions	$\Omega$	DOC (mM)	$P_{\text{CO}_2}$ (kPa)
To analyze the effect of $P_{\text{CO}_2}$ on calcite precipitation at variable $\Omega$	3	1	1-20	0	0.035, 5, 10
To analyze the effect of $P_{\text{CO}_2}$ on calcite precipitation at constant $\Omega$	21	3	5	0	0.035, 2, 3, 4.5, 5, 7, 9, 10
To analyze the effect of DOC on calcite precipitation at 5 kPa	3	1	2.5-2.0	0.07, 0.39, 1.8	5
To analyze the effect of DOC on calcite precipitation at 10 kPa	3	1	2.5-2.0	0.02, 0.48, 3.50	10
To analyze the effect of DOC on crystal growth	4	2	2	0.02-1	5, 10
To analyze the effect of DOC on heterogeneous nucleation	6	2	5	0.05-0.85	0.035, 5, 10

atmospheric partial pressure of  $\text{CO}_2$  ( $P_{\text{CO}_2} = 0.035$  kPa) but concentrations of  $\text{CO}_2$  in the root zone are 10–500 times higher than in the atmosphere. The effect of  $P_{\text{CO}_2}$  on the precipitation rate of calcite in the absence of DOC was measured and modeled by Busenberg and Plummer (1986). They conducted crystal growth experiments by measuring the increase in weight of single crystals suspended in solutions with  $\Omega$  values from 1.5 to 100. However, crystal growth, in solutions far from equilibrium, only accounts for part of the precipitation process. In the absence of DOC and absence of calcite crystals, Lebrón and Suárez (1996) observed precipitation in the bulk solution. It is likely that dust particles in suspension, bacteria, and extraneous agents act as active sites for the calcite to precipitate by heterogeneous nucleation.

The objectives of this study were: (1) To reevaluate the effect of the  $P_{\text{CO}_2}$  on the total calcite precipitation by measuring the amount of Ca and  $\text{HCO}_3^-$  depleted from the solution, (2) To determine the effect of the DOC on crystal growth and heterogeneous nucleation of calcite at different levels of  $P_{\text{CO}_2}$ , and (3) To quantify the effect of  $P_{\text{CO}_2}$  and DOC concentration in a precipitation rate model.

## 2. MATERIALS AND METHODS

Calcite precipitation experiments were performed using 250 mL flasks connected to a pressurized air- $\text{CO}_2$  source by a plastic capillary inserted into the flask's stopper. The gas was presaturated with water by bubbling through three deionized water-filled 1.0-L towers. The composition of the gas bubbled into the flasks was obtained by mixing a  $\text{CO}_2$ -free gas and 100%  $\text{CO}_2$ ; the fluxes of each one of these gases were measured by mass flow controllers (model 825, Edwards High Vacuum International, Wilmington, MA), and the mixture was monitored by a multichannel flow controller (model 1605 also from Edwards).

Every flask contained 80 mL of calcite supersaturated solution and calcite crystals (Baker, Analytical Reagent) with a particle size of 2–20  $\mu\text{m}$  and a total surface area of 2  $\text{m}^2\text{L}^{-1}$  (0.17 g). Calcite saturated solutions were prepared by reacting deionized water with an excess of

53  $\mu\text{m}$  calcite crystals (Mallinckrodt) under 99 kPa  $P_{\text{CO}_2}$ . Later, this solution was bubbled with a gas with a  $P_{\text{CO}_2}$  lower than 99 kPa yielding a calcite supersaturated solution. We diluted this supersaturated solution with DIW to achieve a wide range of  $\Omega$ .

The flasks were shaken at 90 cpm during the experiment on a reciprocating shaker table in a constant temperature room at  $25 \pm 0.5^\circ\text{C}$ . A flask with  $\text{NaHCO}_3$  was used as a blank in each experiment to ensure that evaporation was not occurring.

Samples from the supernatant were taken at different intervals and filtered through pre-rinsed 0.1  $\mu\text{m}$  filters. A portion of the sample was diluted five-fold to avoid further precipitation and analyzed for Ca and alkalinity. The other portion of the sample was acidified with  $\text{HNO}_3$ , bubbled for 5 min with  $\text{O}_2$  and analyzed for DOC with a Dohrmann Carbon Analyzer (Dohrmann, Santa Clara, CA). The pH of the suspensions was measured at the time of sampling with a Fisher Accumet 520 pH meter (Fisher Scientific Co., Pittsburgh, PA) and a Thomas 4094 combination pH electrode (Thomas Scientific, Swedesboro, NJ) calibrated with buffers pH 4.00 and 6.86 to within 0.01 pH units at  $25^\circ\text{C}$ . Calcium was determined by inductively coupled plasma emission spectrometry, alkalinity was measured by titration with  $\text{KH}(\text{IO}_3)_2$  (National Bureau of Standards primary acid standard) as described in Suárez et al. (1992). Precipitation rates were expressed as the amount of Ca and  $\text{HCO}_3^-$  depleted from the solution per time unit. Rates calculated based on Ca data agreed within a 2% difference to the rates calculated from the alkalinity data. The saturation levels for calcite were calculated for every sample from pH and solution composition with the speciation program GEOCHEM-PC (Parker et al., 1994).

Table 1 shows the conditions at which the forty different experiments were conducted, all of them were performed at  $25^\circ\text{C}$ . Specific characteristics for each one of them are explained below.

### 2.1. Calcite Precipitation Rate as Affected by $P_{\text{CO}_2}$ and DOC

The effect of the  $P_{\text{CO}_2}$  on the calcite precipitation rate in the absence of DOC was measured in solutions with 2  $\text{m}^2\text{L}^{-1}$  calcite seeds, at variable and constant  $\Omega$ . Calcite precipitation rate was measured in the range of  $\Omega$  1–20 at  $P_{\text{CO}_2}$  0.035, 5, and 10 kPa, and samples were taken at  $t = 1, 5,$  and  $24$  h. In a separate experiment at constant  $\Omega = 5$ , the precipitation rate of calcite was measured in triplicate reactions at  $P_{\text{CO}_2} = 0.035, 2, 3, 4.5, 5, 7, 9,$  and  $10$  kPa, with samples taken at  $t = 0$  and  $1$  h.

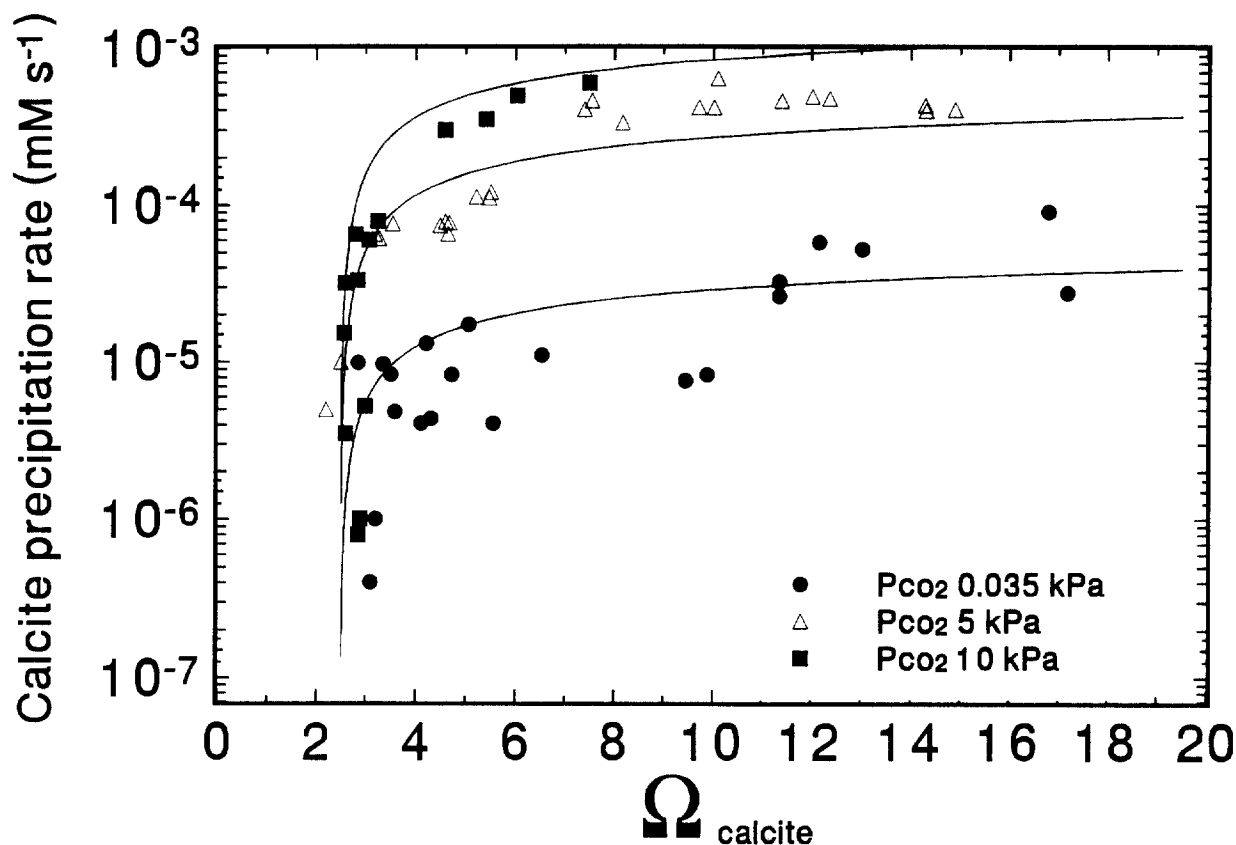


Fig. 1. Calcite precipitation rate as a function of calcite supersaturation for three different partial pressures of  $\text{CO}_2$  in absence of DOC. Solid lines represent the precipitation model proposed in the present work.

Calcium carbonate precipitation rates were also measured in the presence of DOC using calcite seeds ( $2 \text{ m}^2 \text{ L}^{-1}$ ) at  $P_{\text{CO}_2}$  of 5 and 10 kPa, and  $\Omega$  values were varied from 2.5 to 20. Suwannee river fulvic acid reference (International Humic Substances Society, Golden, CO) was added to the reaction vessels to reach 0.07, 0.39, and 1.80 mM for the  $P_{\text{CO}_2} = 5$  kPa experiment, and 0.02, 0.48, and 3.50 mM for the experiment at  $P_{\text{CO}_2} = 10$  kPa. Samples from the supernatant were taken at  $t = 0, 1, 5,$  and  $24$  h. Calcite saturation levels were calculated for each sample taking into account the presence of the Ca-DOC complex. We used the value  $\text{p}K = 1.7$  for the complexation of fulvic acid with Ca corresponding to  $\text{FUL}2^-$  in GEOCHEM-PC. The choice of  $\text{FUL}2^-$  was based on the similarities of the elemental chemical composition and the infrared spectra of this fulvic acid (Sposito et al., 1976) and the Suwannee fulvic acid reference (Lebron and Suarez, 1996) used in the present study.

## 2.2. Calcite Precipitation Mechanisms

We studied the capability of DOC to inhibit calcite precipitation at different  $\text{CO}_2$  concentrations for precipitation conditions of crystal growth and heterogeneous nucleation as follows.

The calcite precipitation rate was measured in duplicate suspensions of calcite seeds ( $2 \text{ m}^2 \text{ L}^{-1}$ ) with  $\Omega = 2$  and  $P_{\text{CO}_2} = 5$  and 10 kPa. Under these conditions precipitation is only by crystal growth (Lebron and Suarez, 1996). Suwannee river fulvic acid reference was added to achieve DOC concentrations from 0.02 to 1 mM. Ca-DOC complexation was accounted for to maintain the same  $\Omega$  value in all the flasks. Samples from the supernatant were taken at 0 and 1 h and analyzed for Ca, alkalinity, and DOC. The difference between the initial DOC and the DOC after the reaction was considered the adsorbed DOC on the calcite crystals. Solutions with no precipitation after 1 h were sampled at different intervals for three days. Standard errors of the duplicates for

the Ca and alkalinity analyses were within  $\pm 0.02 \text{ mmol}_c \text{ L}^{-1}$  and DOC within  $\pm 0.005 \text{ mM}$ .

Suwannee river fulvic acid was added to a solution with  $\Omega = 5$  to reach six concentrations varying from 0.05 to 0.85 mM in DOC. Reactions were run in duplicate. Calcite crystals were coated with an amount of DOC necessary to avoid precipitation of calcite by crystal growth ( $C_{\text{inh}}$  from Table 3) and added to the solutions. Supernatant samples were taken at 0 and 1 h. Solutions with no precipitation after 1 h were sampled at intervals for three days. Precipitation rates were measured at  $P_{\text{CO}_2} = 0.035, 5,$  and  $10$  kPa. We then calculated the decrease in precipitation rate with increasing DOC as explained above.

## 3. RESULTS

### 3.1. Calcite Precipitation as Affected by $P_{\text{CO}_2}$ in the Absence of DOC

The calcite precipitation rates measured at different  $P_{\text{CO}_2}$  and variable  $\Omega$  are shown in Fig. 1. The precipitation rate increased with increasing  $\Omega$  and increasing  $P_{\text{CO}_2}$ . As shown in Fig. 2, for a constant  $\Omega = 5$ , the precipitation of calcite increased linearly with increasing  $P_{\text{CO}_2}$ . Also shown is the standard deviation for the measured precipitation rates for each  $P_{\text{CO}_2}$  and the linear equation that relates the  $P_{\text{CO}_2}$  and the precipitation rate for the range of  $\text{CO}_2$  studied.

The activities of different species in solution at each level of  $P_{\text{CO}_2}$  is shown in Table 2. Figure 3 gives the relationship between measured calcite precipitation rates and the activity of the  $\text{CaHCO}_3^+$  species in solution for constant  $\Omega$  and varying

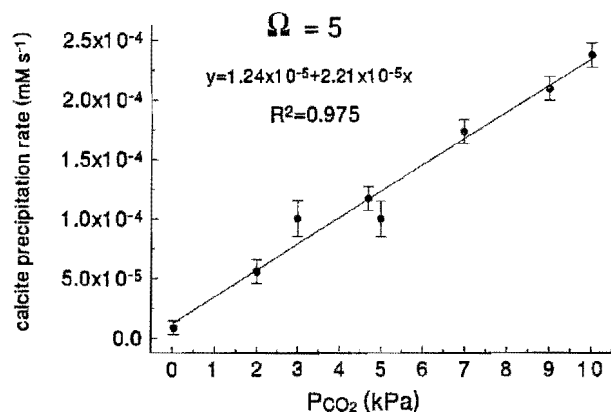


Fig. 2. Calcite precipitation rate, with standard errors, at constant supersaturation level ( $\Omega=5$ ) as a function of the partial pressure of  $\text{CO}_2$  in the absence of DOC.

$P_{\text{CO}_2}$ . Since the speciation of the chemical components of the solutions are in equilibrium with the speciation on the surface of the mineral, the linear relationship between precipitation rate and  $\text{CaHCO}_3^+$  at constant  $\Omega$  shown in Fig. 3 suggests that  $\text{CaHCO}_3^+$  has an active role in the precipitation of calcite. The measured pH, precipitation rate, and ionic strength are also shown in Table 2.

### 3.2. Calcite Precipitation as Affected by $P_{\text{CO}_2}$ in the Presence of DOC

The decrease in the calcite precipitation rate with increasing DOC at  $P_{\text{CO}_2} = 5$  kPa and 10 kPa is shown in Figs. 4 and 5. Near equilibrium, the  $\Omega$  value at which the precipitation rate was undetectable increased when the DOC concentration increased for the same  $P_{\text{CO}_2}$ . At  $P_{\text{CO}_2} = 10$  kPa and DOC = 3.50 mM no precipitation was detected below  $\Omega = 4$ .

Calcite precipitation rate at  $P_{\text{CO}_2} 0.035$  kPa with the addition of DOC in the presence of calcite crystals was not measured because we already established that when  $\text{DOC} \geq 0.05$  mM the precipitation rate is independent of the calcite surface area (Lebrón and Suárez, 1996). The calcite precipitation rate at  $P_{\text{CO}_2} 0.035$  kPa and different levels of DOC in the absence of

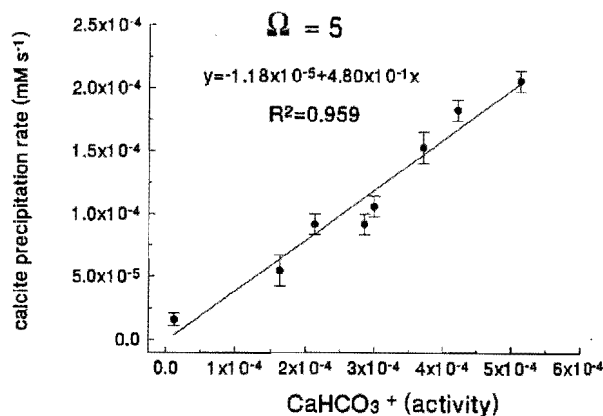


Fig. 3. Calcite precipitation rate, with standard errors, at constant supersaturation level ( $\Omega=5$ ) as a function of  $\text{CaHCO}_3^+$  activity in the absence of DOC.

calcite crystals was previously measured by Lebrón and Suárez (1996).

#### 3.2.1. Calcite crystal growth

In the absence of calcite crystals, solutions with  $\Omega = 2$  remained metastable for several days. This observation indicates that heterogeneous nucleation is not a significant precipitation mechanism under these conditions. The precipitation rates of calcite at  $\Omega = 2$  in the presence of calcite seeds, different DOC concentrations, and  $P_{\text{CO}_2}$  values of 5 and 10 kPa are shown in Fig. 6, also shown are the error bars in the horizontal and vertical axes. The amount of adsorbed DOC (in  $\text{mmol m}^{-2}$ ) necessary to inhibit the precipitation rate of calcite by crystal growth ( $C_{\text{inh}}$ ) increased with increasing  $P_{\text{CO}_2}$ . Note that the relevance of Fig. 6 is the value of  $C_{\text{inh}}$  at which the precipitation rate is  $\leq 10^{-8}$   $\text{mM s}^{-1}$ , which is the detection limit for this experiment.

We calculated the Langmuir adsorption isotherm for DOC expressed as

$$C_{\text{ads}} = K M \text{DOC} / (1 + K \text{DOC}) \quad (1)$$

Table 2. Supersaturation level ( $\Omega$ ), pH, calcite precipitation rate (R), and activity of the species in solution at different partial pressures of  $\text{CO}_2$  ( $P_{\text{CO}_2}$ ).

$P_{\text{CO}_2}$ (kPa)	$\Omega^\dagger$	Ionic Strength	pH	R ( $\text{mM s}^{-1}$ )	$\text{HCO}_3^-$	$\text{H}_2\text{CO}_3(\text{aq})$	$\text{CaHCO}_3^+$	$\text{CaCO}_3^*(\text{aq})$
0.035	5.11	$2.7 \times 10^{-3}$	8.50	$8.75 \times 10^{-6}$	$1.63 \times 10^{-3}$	$1.16 \times 10^{-5}$	$1.20 \times 10^{-5}$	$2.43 \times 10^{-5}$
2	4.92	$1.1 \times 10^{-2}$	7.34	$5.56 \times 10^{-5}$	$6.67 \times 10^{-3}$	$6.85 \times 10^{-4}$	$1.63 \times 10^{-4}$	$2.28 \times 10^{-6}$
3	5.01	$1.3 \times 10^{-2}$	7.23	$1.00 \times 10^{-4}$	$7.74 \times 10^{-3}$	$1.03 \times 10^{-3}$	$2.13 \times 10^{-4}$	$2.32 \times 10^{-5}$
4.7	5.05	$1.5 \times 10^{-2}$	7.10	$1.17 \times 10^{-4}$	$9.10 \times 10^{-3}$	$1.61 \times 10^{-3}$	$2.86 \times 10^{-4}$	$2.33 \times 10^{-5}$
5	5.36	$1.6 \times 10^{-2}$	7.16	$1.00 \times 10^{-4}$	$9.33 \times 10^{-3}$	$1.72 \times 10^{-3}$	$3.00 \times 10^{-4}$	$2.35 \times 10^{-5}$
7	5.09	$1.8 \times 10^{-2}$	6.99	$1.73 \times 10^{-4}$	$1.05 \times 10^{-2}$	$2.40 \times 10^{-3}$	$3.71 \times 10^{-4}$	$2.34 \times 10^{-5}$
9	4.82	$1.9 \times 10^{-2}$	6.91	$2.09 \times 10^{-4}$	$1.13 \times 10^{-2}$	$3.10 \times 10^{-3}$	$4.22 \times 10^{-4}$	$2.22 \times 10^{-5}$
10	5.12	$2.0 \times 10^{-2}$	6.88	$3.10 \times 10^{-4}$	$1.23 \times 10^{-2}$	$3.69 \times 10^{-3}$	$5.13 \times 10^{-4}$	$2.47 \times 10^{-5}$

$\dagger \Omega = (IAP/K_{\text{SP}})$

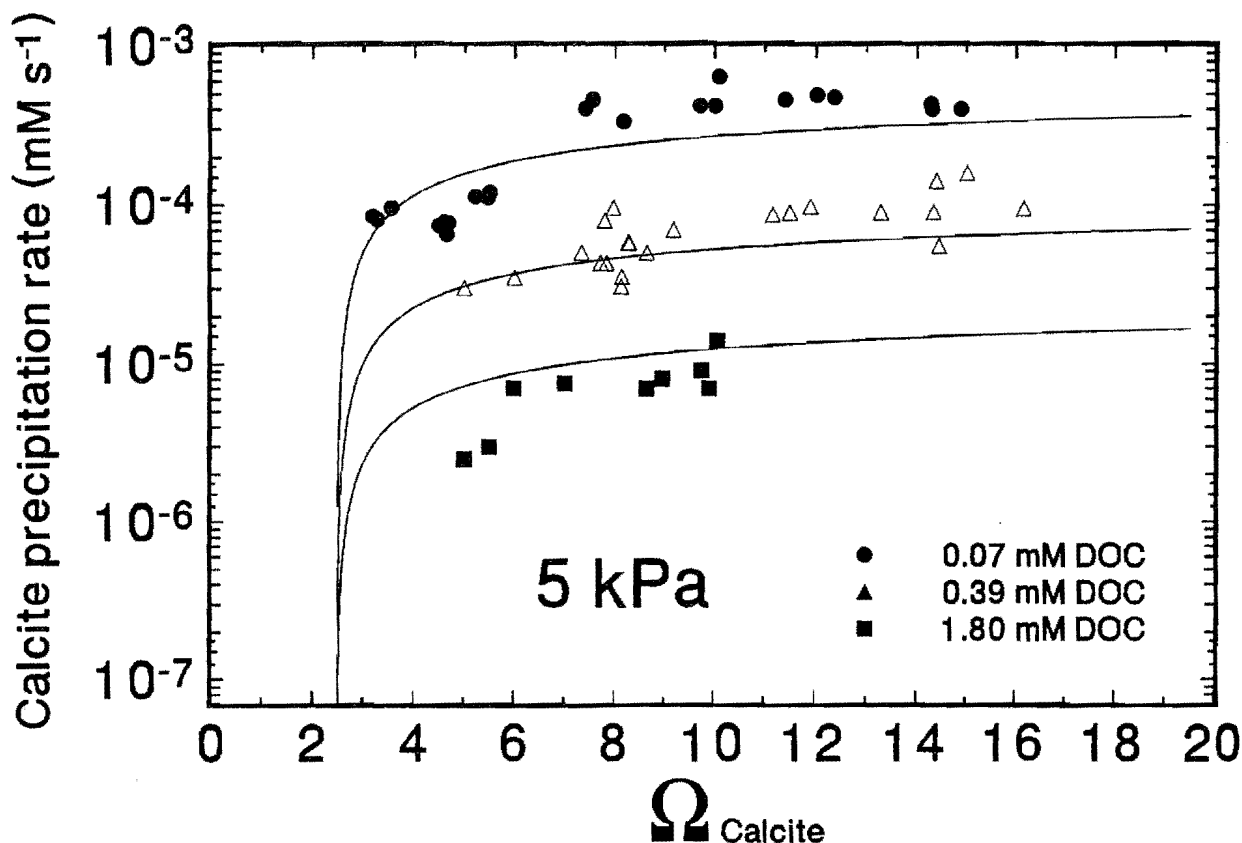


Fig. 4. Calcite precipitation rate as a function of calcite supersaturation for  $P_{\text{CO}_2} = 5$  kPa and dissolved organic carbon (DOC) concentrations of 0.07, 0.39, and 1.80 mM.

where  $C_{\text{ads}}$  is the amount of DOC adsorbed on the surface of the calcite crystals,  $K$  is an affinity parameter, and  $M$  is the adsorption maximum. We calculated the adjustable parameters,  $K$  and  $M$ , using our experimental data and the program ISOTHERM (Kinniburgh, 1986; Table 3). Figure 7 shows the experimental data (values for 0.035 kPa in this section are taken from Lebron and Suarez, 1996) and calculated isotherms represented as solid lines. From Fig. 7, we calculated the DOC in equilibrium with the  $C_{\text{inh}}$ , these values for the three  $P_{\text{CO}_2}$  are also shown in Table 3. DOC concentration in equilibrium with  $C_{\text{inh}}$  is related to the  $P_{\text{CO}_2}$  by the logarithmic function:  $\text{DOC} = 0.14 + 0.06 \log P_{\text{CO}_2}$  ( $R^2 = 0.9999$ ).

We also calculated the relative decrease in the calcite precipitation rate with increasing DOC. This factor was obtained by dividing the precipitation rates of calcite at different concentrations of DOC by the precipitation rate of calcite in the absence of DOC. The fractional decrease in the precipitation rate of calcite (precipitation rate reduction) calculated for the three levels of  $P_{\text{CO}_2}$  as a function of the DOC, is presented in Fig. 8.

### 3.2.2. Calcite heterogeneous nucleation

Supersaturated solutions with  $\Omega = 5$  do not remain metastable for long periods of time. Precipitation by heterogeneous nucleation occurs within hours in the absence of calcite crystals

or in the presence of DOC-coated crystals. The precipitation rate by heterogeneous nucleation decreased when DOC increased and when the  $P_{\text{CO}_2}$  decreased. The decrease in the precipitation rate of calcite for  $P_{\text{CO}_2}$  0.035, 5, and 10 kPa as a function of the DOC is presented in Fig. 9.

## 4. DISCUSSION

### 4.1. Calcite Precipitation Rate as Affected by $P_{\text{CO}_2}$ in the Absence of DOC

In the  $\Omega$  range of 2–20 we found an increase in the calcite precipitation rate with increasing  $P_{\text{CO}_2}$ , in qualitative agreement with the model of Plummer et al. (1978). However, in the absence of DOC the model of Plummer et al. (1978; also called Plummer-Wigley-Parkhurst equation or PWP equation) underpredicts our measured precipitation rates. The deviation of the PWP equation from our measurements may be due to the implicit assumption of the PWP model, which is that crystal growth is the only mechanism for calcite precipitation. This model was developed by Plummer et al. (1978) from dissolution data and includes a term for the back reaction of crystal growth. The model was evaluated for precipitation data by Plummer et al. (1979), Reddy et al. (1981), Dreybrodt (1981), Suarez (1983), Inskeep and Bloom (1985), Busenberg and Plummer (1986), and Shiraki and Brantley (1995) among others. The agreement between

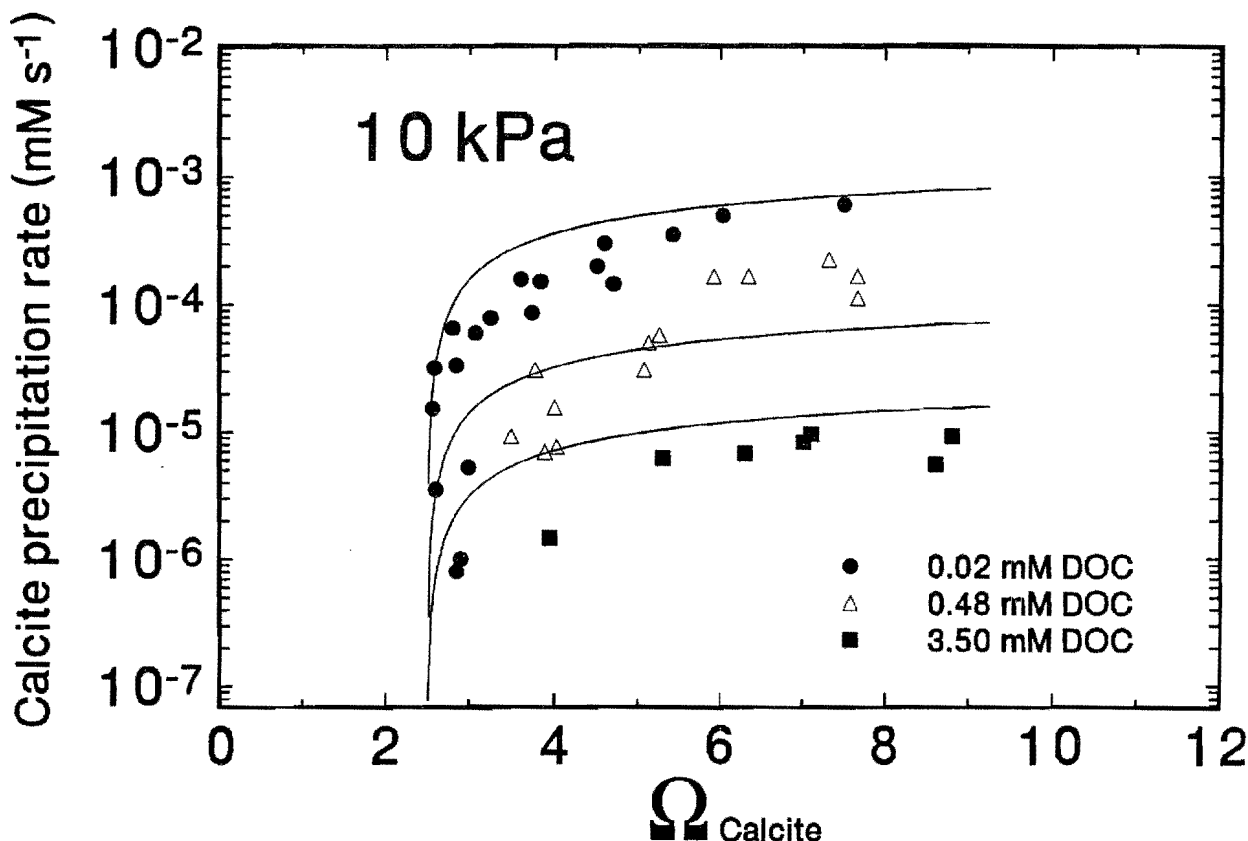


Fig 5. Calcite precipitation rate as a function of calcite supersaturation for  $P_{\text{CO}_2} = 10$  kPa and dissolved organic carbon (DOC) concentrations of 0.02, 0.48, and 3.50 mM.

the measured data from the different authors and the calculated precipitation rates with the PWP model was within the same order of magnitude but varied depending upon the initial conditions of the system. Only Busenberg and Plummer (1986) found an accurate fit between their data and the PWP model in the range of  $\Omega$  1.5–100; however, this good agreement can be attributed to the experimental method. They determined precipitation by the increase in weight of an existing crystal, which measures only precipitation by crystal growth and did not do systematic analyses of the changes in solution composition. Measurement of changes in solution composition would result in determination of overall precipitation rates (crystal growth plus heterogeneous nucleation).

In the absence of calcite crystals, precipitation occurs in supersaturated solutions far from equilibrium. Bacteria and particles in suspension may act as active sites for heterogeneous calcite nucleation. On the other hand, solutions close to equilibrium,  $\Omega \approx 2$ , remain metastable for several days in the absence of calcite crystals, indicating that heterogeneous nucleation does not contribute significantly to calcite precipitation under these conditions (Lebrón and Suárez, 1996).

We observed that at  $\Omega$  values of 3–4 the precipitation increases rapidly, and when  $\Omega = 5$ , there is an inflection in the curve where increases in  $\Omega$  do not yield major changes in the precipitation rate (Fig. 1). At this supersaturation level ( $\Omega > 5$ )

both crystal growth and heterogeneous nucleation are active (Lebrón and Suárez, 1996). Analysis of eight  $P_{\text{CO}_2}$  levels at  $\Omega = 5$  to quantify the effect of  $P_{\text{CO}_2}$  on calcite precipitation in the presence of heterogeneous nucleation suggested that precipitation and  $P_{\text{CO}_2}$  were not independent variables.

PWP model predicts a linear relationship between crystal growth and  $P_{\text{CO}_2}$ ; the fact that precipitation rate in Fig. 2 has a linear relationship with increasing  $P_{\text{CO}_2}$  in the presence of heterogeneous nucleation indicates that heterogeneous nucleation also follows a linear relationship with  $P_{\text{CO}_2}$ . The mechanistic model for the precipitation of  $\text{CaCO}_3$  proposed by Plummer et al. (1978) considers the reaction between bulk solution  $\text{CaHCO}_3^+$  and negative surface sites. Our results (Fig. 3) show that the increase of the precipitation rate of calcite with increases in  $\text{CaHCO}_3^+$  activity remains linear. This linearity may indicate that the  $\text{CaHCO}_3^+$  species has an active role in heterogeneous nucleation as well as in crystal growth, since at  $\Omega = 5$  both precipitation mechanisms are active.

The density of negative charge on the carbonate surface increases when the  $P_{\text{CO}_2}$  increases (Charlet et al., 1990). This increase occurs at  $\text{pH} > \text{pH}_{\text{ZPC}}$  (pH of zero point of charge) and is due to changes in surface speciation. The  $\text{pH}_{\text{ZPC}}$  for calcite has been reported in the literature with values ranging from 7.0 to 10.8 (e.g., Somasundaran and Agar, 1967; Mishra, 1978; Amankonah and Somasundaran, 1985; Thompson and Pownall, 1989; van Capellen et al., 1993). The relatively high solubility of this mineral and the

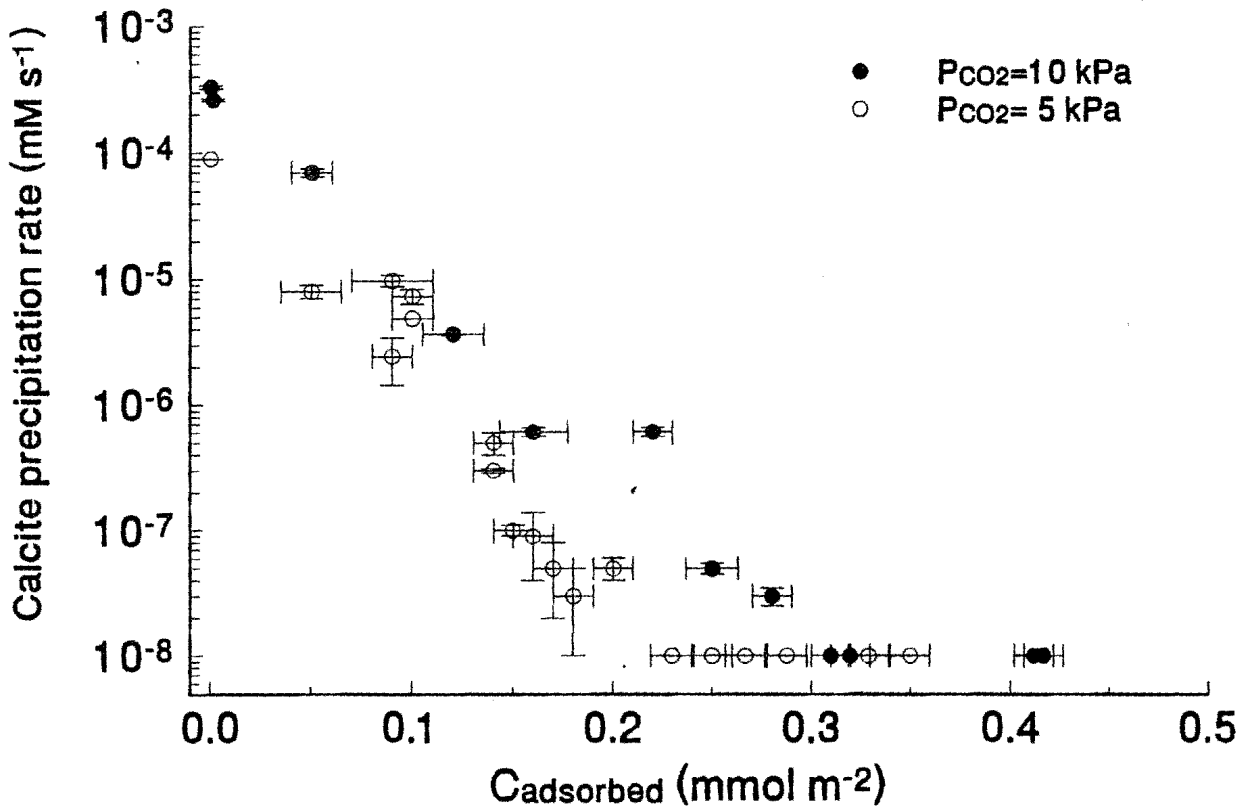


Fig. 6. Calcite precipitation rate by crystal growth ( $\Omega=2$ ) as a function of dissolved organic carbon (DOC) adsorbed on the surface of the crystals.

complexity of carbonate surface speciation make it difficult to accurately determine the  $pH_{ZPC}$  for calcite. The speciation of the chemical components in solution, and on the surface of the mineral, are not uniquely determined by pH alone. This is demonstrated by the shift in  $pH_{ZPC}$  of another carbonate mineral, rhodochrosite, induced by changes in  $P_{CO_2}$  (van Capellen et al., 1993).

In our case, the increase of negative surface charge, together with the increase in the  $CaHCO_3^+$  activity in solution may explain the increase in precipitation by crystal growth with increasing  $P_{CO_2}$ . For heterogeneous nucleation and from Fig. 3, the increase in  $CaHCO_3^+$  alone may also explain an increase in precipitation with increasing  $P_{CO_2}$ . The unknown nature of the active sites in suspension makes it difficult to predict the effect of  $P_{CO_2}$  on the suspended entities; however, in the absence of DOC, crystal growth is important once heterogeneous nucleation causes formation of calcite nuclei.

#### 4.2. Precipitation Rate of Calcite as Affected by $P_{CO_2}$ in the Presence of DOC

The precipitation rate of calcite in the range of  $\Omega = 2.5-20$  decreased when the DOC concentration increased for  $P_{CO_2} = 5$  and  $P_{CO_2} = 10$  kPa (Figs. 4 and 5); however, higher DOC concentrations were needed to cause an equal reduction in precipitation when the  $P_{CO_2}$  increased. In the presence of DOC, precipitation rates were below our detection limit when  $\Omega \approx 2$ . In a region near equilibrium the surface charge of carbonate minerals remains relatively close to zero (Charlet et al., 1990). The coating by DOC at low negative surface charge when  $\Omega$  is close to 1 explains the reduction of the precipitation rate to levels close to zero even when the system is still supersaturated. This reduction of the precipitation rate near equilibrium is consistent with the persistence of supersaturated conditions observed in

Table 3. Langmuir isotherm parameters for three  $P_{CO_2}$  values, amount of DOC necessary to inhibit crystal growth ( $C_{inh}$ ) and DOC in equilibrium with  $C_{inh}$  ( $DOC_{eq}$ ).

$P_{CO_2}$ (kPa)	K ( $mmol^{-1} L$ )	M ( $mmol m^2$ )	$C_{inh}$ ( $mmol m^2$ )	$DOC_{eq}$ (mM)
0.035	20.0	0.20	0.10	0.05
5	29.0	0.28	0.23	0.16
10	64.9	0.34	0.31	0.16

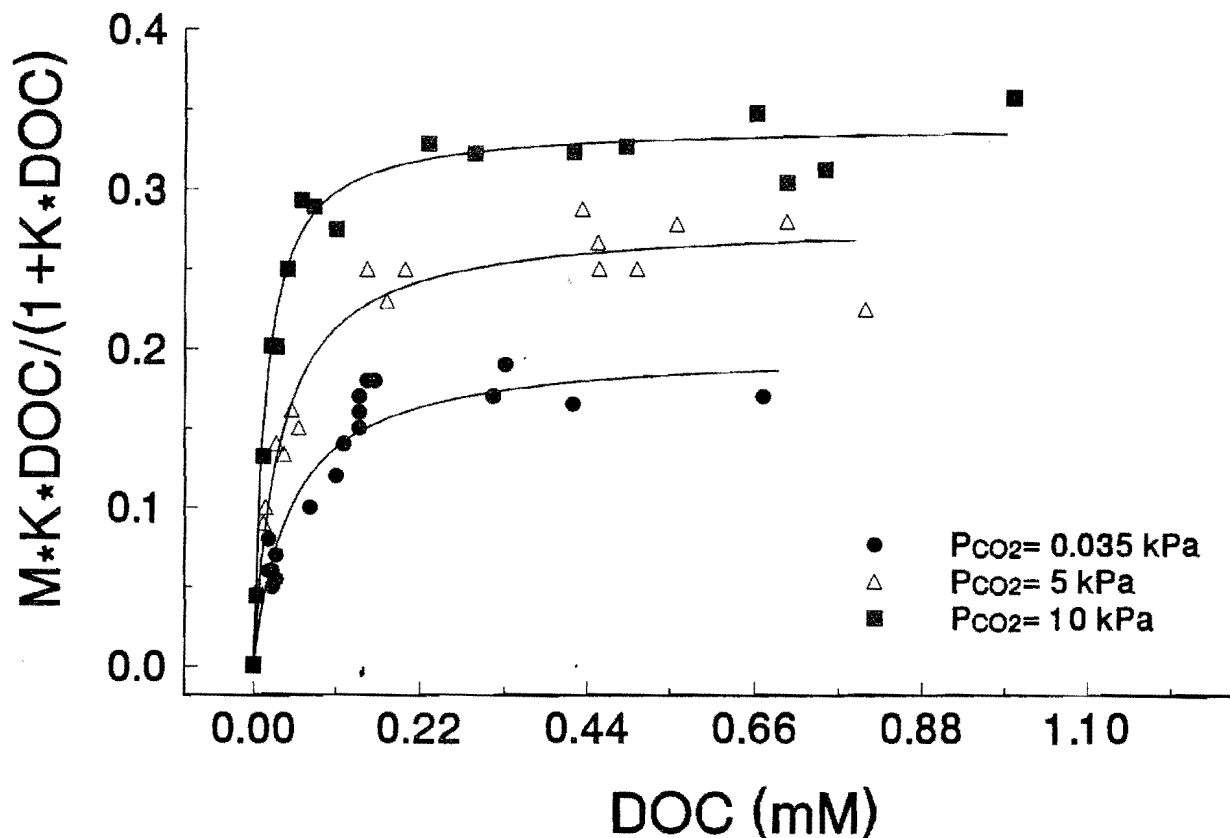


Fig. 7. Langmuir adsorption isotherms for dissolved organic carbon (DOC) adsorbed on calcite at three different partial pressures of  $\text{CO}_2$ . ( $C_{\text{ads}} = M K \text{ DOC} / (1 + K \text{ DOC})$ , where  $M$  is the maximum adsorption and  $K$  is the affinity constant.)

natural systems by many researchers (Back and Hanshaw, 1970; Jacobson and Uzdowski, 1975; Reynolds, 1978; Suarez, 1977, 1983; Suarez and Rhoades, 1982; Dandurand et al., 1982; Last, 1982; Inskeep and Bloom, 1986; Lorah and Herman, 1988; Suarez et al., 1992) and corresponds to metastable supersaturated levels with respect to calcite.

At atmospheric  $P_{\text{CO}_2}$ , Lebron and Suarez (1996) have shown that crystal growth and heterogeneous nucleation are both affected by the presence of DOC. However, the quantification of the reduction of calcite precipitation due to DOC has to be evaluated at different  $P_{\text{CO}_2}$  levels because the amount of DOC necessary to coat calcite crystals (for the same surface area) changes with the  $P_{\text{CO}_2}$ . With increasing  $P_{\text{CO}_2}$ , the negative charge density on the crystals increases, which will affect crystal growth. Also these increases in  $P_{\text{CO}_2}$  are associated with a decrease in the solution pH and increase in the ionic strength at constant  $\Omega$ . Solution pH and ionic strength are known to affect the structure and reactivity of the DOC which may have repercussions on the inhibition of crystal growth and heterogeneous nucleation.

#### 4.2.1. Calcite crystal growth

Calcite precipitation in supersaturated solutions at  $\Omega = 2$  where crystal growth is the dominant mechanism was measured at  $P_{\text{CO}_2} = 5$  and  $P_{\text{CO}_2} = 10$  kPa in the presence of different DOC concentrations. Calcite precipitation decreased rapidly as

more DOC covered the crystal surfaces at both  $P_{\text{CO}_2}$  levels (Fig. 6). Higher concentrations of DOC were necessary, at 5 kPa, to inhibit calcite precipitation in comparison with  $P_{\text{CO}_2} = 0.035$  kPa (Lebron and Suarez, 1996) and even more DOC was necessary when the  $P_{\text{CO}_2}$  was 10 kPa (Fig. 6). The Langmuir isotherm in Fig. 7 and Table 3 show more clearly the increase in the adsorption maximum and the affinity parameter with  $P_{\text{CO}_2}$ . Table 3 indicates that it is not necessary to completely coat the calcite crystals with a monolayer of DOC to inhibit crystal growth, especially at  $P_{\text{CO}_2} = 0.035$  kPa. The precipitation rate at atmospheric conditions was reduced to below our detection limit when half of the total surface area was covered by DOC.

The fact that at constant  $\Omega$  a greater DOC concentration is required to block the active sites on the calcite crystals with increasing  $P_{\text{CO}_2}$  may be due to a combination of at least three different factors: (1) the increase in negative charge on the calcite surface with increasing  $P_{\text{CO}_2}$  (Charlet et al., 1990), (2) the decrease of the bonding capacity of the fulvic acid with decreasing pH of the solution (Engelbreton et al. 1996), and (3) the decrease in the specific volume of the DOC due to increase in the ionic strength of the solutions (Benedetti et al., 1996).

The solution pH decreases when  $P_{\text{CO}_2}$  increases (Table 2). The degree of dissociation of the organic matter functional groups depends largely on the pH of the solution. At higher pH, the mutual repulsion of the negatively charged sites causes the

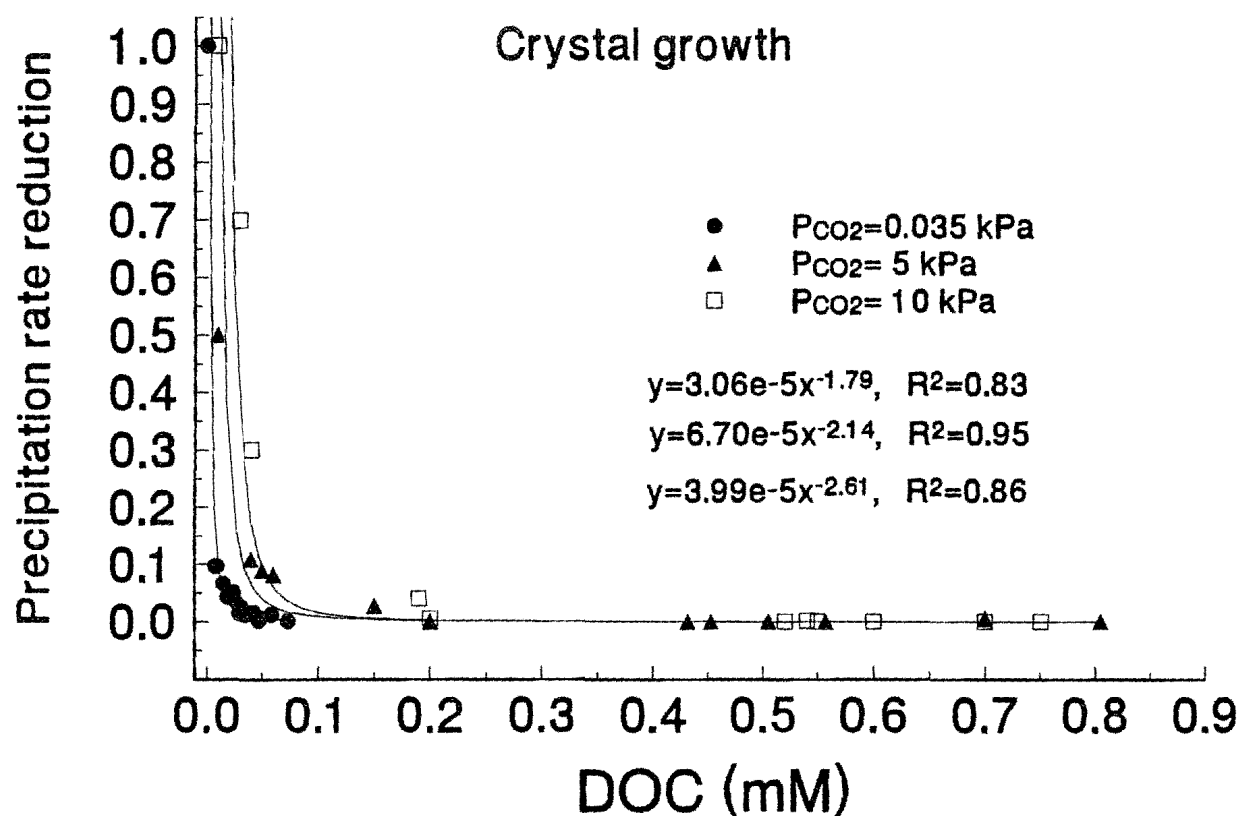


Fig. 8. Reduction in the rate of calcite precipitation by crystal growth as a function of dissolved organic carbon (DOC) at three different partial pressures of  $CO_2$ . Calculations were made by dividing the precipitation rates of calcite at different DOC levels by the precipitation rate of calcite in the absence of DOC.

molecule with multiple functional groups to adopt a stretched configuration. As the pH of the solution is lowered and some of the charged sites are neutralized, a reduction in intramolecular repulsion is predicted resulting in a contraction of the polymer chain. Engebretson et al. (1996) defined an association index for humic acids using fluorescence anisotropy. This association index is a quantitative parameter for estimating the polymer contraction. They found that the association index increases with decreasing pH, consistent with a structural contraction of the humic acid molecule. Another factor affecting the characteristics of DOC is the ionic strength. Murphy and Zachara (1995) and Benedetti et al. (1996) found that the specific volume of humic substances is strongly dependent on the ionic strength. Several attempts have been made to model electrostatic interactions of humic substances with organic ligands and cations (Tipping and Hurley, 1992; Marinsky and Ephraim, 1986; De Wit et al., 1990, 1993; Bartschart et al., 1992; Barak and Chen, 1992; and Milne et al., 1995). The general consensus is that the binding capability of humic substances generally decreases with decreasing pH and increasing salt concentration. We observed a decrease in pH and an increase in ionic strength when the  $P_{CO_2}$  increased for the same  $\Omega$  value (Table 2) which may account for the lower reactivity of fulvic acid with the calcite crystal surface with increasing  $P_{CO_2}$ . Additionally, the increased negative charge of the calcite crystals, with increasing  $P_{CO_2}$ , offers more reactive sites for crystal growth.

#### 4.2.2. Calcite heterogeneous nucleation

The precipitation rate of calcite at  $\Omega = 5$  and in the presence of DOC coated crystals decreased rapidly with increasing DOC at  $P_{CO_2}$  0.035, 5, and 10 kPa (Fig. 9). The decrease in precipitation rate was described by an exponential function (Fig. 9) and was higher at higher  $P_{CO_2}$  for the same concentration of DOC. The effect of pH and ionic strength on the DOC and their effects on the inhibition of calcite precipitation by heterogeneous nucleation are similar to their effects on the inhibition of calcite precipitation by crystal growth, discussed above.

#### 4.3. Precipitation Rate Equation

Calcite precipitation rate in the presence of fulvic and humic substances and atmospheric  $P_{CO_2}$  has been represented by the following expression (Lebron and Suarez, 1996):

$$R_T = R_{CG} + R_{HN} \quad (2)$$

where  $R_T$  is the total precipitation rate of calcium carbonate ( $mM s^{-1}$ ),  $R_{CG}$  is the calcite precipitation rate due to crystal growth, and  $R_{HN}$  is the precipitation rate due to heterogeneous nucleation.

For atmospheric conditions, the effect of DOC on the calcite precipitation rate was quantified by a factor called precipitation rate reduction, ( $f(DOC)$ ), which is the fractional decrease in the calcite precipitation rate when DOC is added to the solution. In

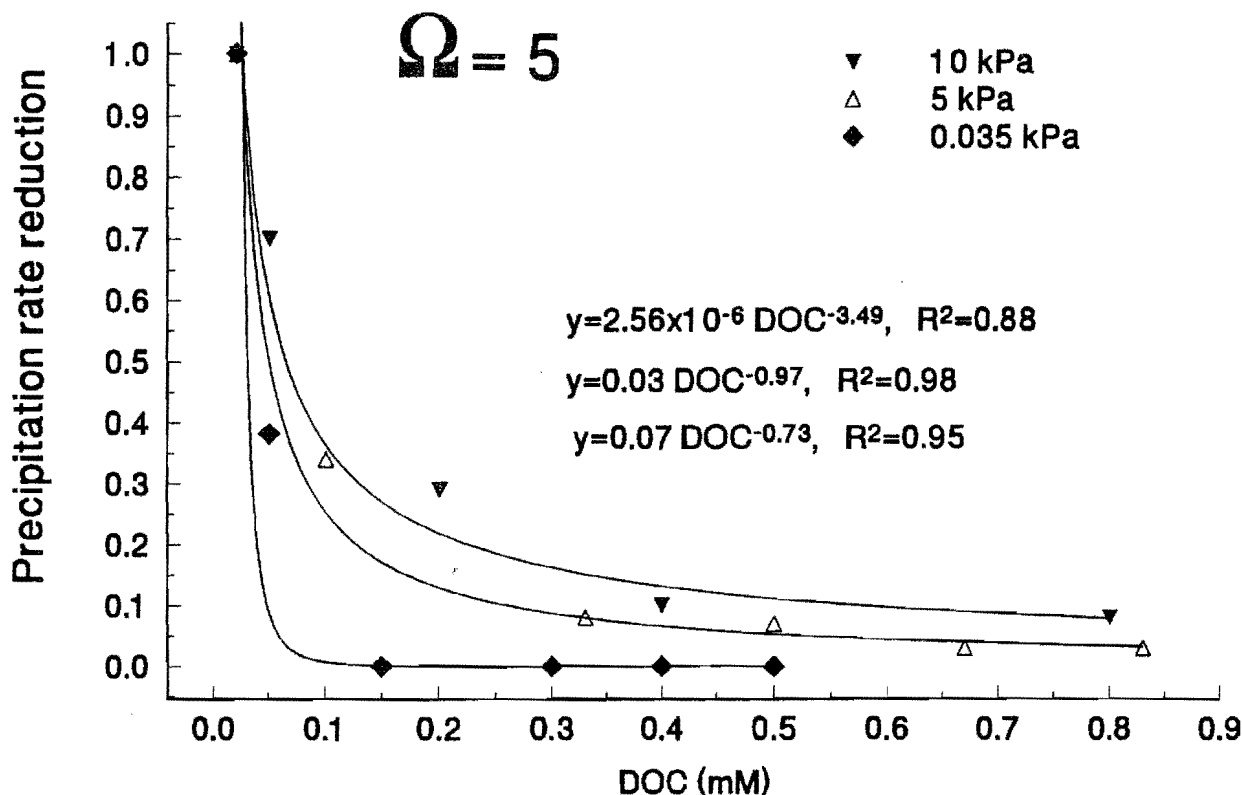


Fig. 9. Reduction in the rate of calcite precipitation by heterogeneous nucleation as a function of dissolved organic carbon (DOC) at three different partial pressures of  $\text{CO}_2$ . Calculations were made by dividing the precipitation rates of calcite at different DOC levels by the precipitation rate of calcite in the absence of DOC.

the present study, the precipitation rate reduction factor followed an exponential curve at the three  $P_{\text{CO}_2}$  levels studied for both precipitation mechanisms (Figs. 8 and 9). Since the inhibition of the DOC is itself dependent on the  $P_{\text{CO}_2}$ , we modeled the new rate reduction ( $f(\text{DOC}, P_{\text{CO}_2})$ ) as follows:

$$f(\text{DOC}, P_{\text{CO}_2}) = \alpha \text{DOC}^\beta \quad (3)$$

where

$$\alpha = \psi P_{\text{CO}_2} \quad (4)$$

and

$$\beta = \theta + \lambda \log(P_{\text{CO}_2} + 1) \quad (5)$$

where  $\psi$  ( $\text{kPa}^{-1} \text{mmol}^{-1} \text{L}$ ),  $\beta$  (a-dimensional),  $\theta$  (a-dimensional), and  $\lambda$  ( $\log \text{kPa}^{-1}$ ) are constants. Substituting Eqns. 4 and 5 into Eqn. 3 and taking logarithms we obtain

$$\log(f(\text{DOC}, P_{\text{CO}_2})) = \log \psi + \log P_{\text{CO}_2} + \theta \log \text{DOC} + \lambda (\log(P_{\text{CO}_2} + 1)) \log \text{DOC} \quad (6)$$

where all the variables are known for the experimental data for crystal growth (Fig. 8). Using least squares, the calculated constants for crystal growth are  $\psi = 8.57 \times 10^{-6}$ ,  $\theta = -3.052 \pm 0.168$ , and  $\lambda = 0.793 \pm 0.202$ . The fit of Eqn. 6 to the data gave an  $R^2 = 0.904$ .

The term  $R_{\text{CG}}$  ( $\text{mmol L}^{-1} \text{s}^{-1}$ ), with the incorporation of the effect of  $P_{\text{CO}_2}$ , has the following form:

$$R_{\text{CG}} = s k_{\text{CG}} ([\text{Ca}^{2+}][\text{CO}_3^{2-}] - K_{\text{SP}}) f(\text{DOC}, P_{\text{CO}_2})_{\text{CG}} \quad (7)$$

where brackets represent activities,  $s$  is the calcite surface area ( $\text{m}^2 \text{L}^{-1}$ ),  $k_{\text{CG}}$  is the precipitation rate constant for crystal growth ( $\text{L}^2 \text{mmol}^{-1} \text{m}^{-2} \text{s}^{-1}$ ), and  $K_{\text{SP}}$  is the solubility product of pure calcite at  $25^\circ\text{C}$ . For our experimental conditions,  $k_{\text{CG}} = 64.8 \text{L}^2 \text{mmol}^{-1} \text{s}^{-1} \text{m}^{-2}$ , and  $f(\text{DOC}, P_{\text{CO}_2})_{\text{CG}}$  is the precipitation rate reduction factor. This factor varies from 1 to 0, where 1 represents the precipitation rate of calcite when  $\text{DOC} = 0$ . The term  $f(\text{DOC}, P_{\text{CO}_2})$  is zero when  $\text{DOC} \geq 0.14 + 0.06 \log P_{\text{CO}_2}$ . This expression represents the amount of DOC as a function of the  $P_{\text{CO}_2}$  needed to totally inhibit calcite crystal growth by coating of the crystal surfaces.

The precipitation rate for heterogeneous nucleation is represented by the following expression:

$$R_{\text{HN}} = k_{\text{HN}} f(\text{SA}) (\log(\Omega - 1.5)) f(\text{DOC}, P_{\text{CO}_2})_{\text{HN}} \quad (8)$$

where  $k_{\text{HN}}$  is the precipitation rate constant ( $\text{mmol s}^{-1} \text{m}^{-2}$ ). For heterogeneous nucleation,  $k_{\text{HN}} = 7.82 \times 10^{-4}$ . The  $f(\text{SA})$  term is for the active sites ( $\text{m}^2 \text{L}^{-1}$ ) (heterogeneous nucleation) of the particles in suspension,  $f(\text{SA}) \geq 1$ , where  $f(\text{SA}) = 1$  in the absence of particles in suspension. The value 1.5 has been chosen since no precipitation was observed below  $\Omega \approx 2.5$ , the term  $\log(\Omega - 1.5)$  has positive values when  $\Omega > 2.5$  and  $f(\text{DOC}, P_{\text{CO}_2})$  is the percentage decrease in the precipitation rate due to the presence of DOC. From the experimental data in Fig. 9, Eqn. 6, and following the same procedure as with crystal

growth, the constants defining  $f(\text{DOC}, P_{\text{CO}_2})$  have the following values:  $\psi = 5.916 \times 10^{-3}$ ,  $\theta = -1.41 \pm 0.27$ , and  $\lambda = 0.61 \pm 0.28$ , with  $R^2 = 0.965$  ( $p < 0.001$ ). The substitution of Eqn. 7 and Eqn. 8 into Eqn. 1 predicts the calcite precipitation rate in the range of  $0 \leq \text{DOC} \leq 3.5 \text{ mM}$  and  $0.035 \leq P_{\text{CO}_2} \leq 10 \text{ kPa}$ .

#### 4.4. Prediction of the Calcite Precipitation Rate in Natural Systems

Using the mathematical model presented above we estimated the precipitation rate of calcite at  $\text{DOC} = 0.07, 0.39, \text{ and } 1.80 \text{ mM}$  at  $5 \text{ kPa}$ , and  $\text{DOC} = 0.02, 0.48, \text{ and } 3.50 \text{ mM}$  at  $10 \text{ kPa}$ . The model presented showed good agreement with the experimental data, (Figs. 1, 4, and 5, solid lines). This new model should result in more realistic predictions of calcite precipitation rates and solution composition in near surface environments such as soils and shallow aquifers.

### 5. CONCLUSIONS

In solutions with  $\Omega \geq 5$  and in the absence of DOC, heterogeneous nucleation should be considered as a separate mechanism of calcite precipitation in addition to crystal growth. Previous models fail to account for the precipitation outside the initial crystals, yielding a poor agreement with our experimental results.

The incorporation of  $\text{CaHCO}_3^+$  into the negatively charged calcite surface crystal has been confirmed as the mechanism of calcite precipitation by crystal growth. When crystal growth and heterogeneous nucleation were active, the linearity between precipitation rate and  $\text{CaHCO}_3^+$  holds, indicating that heterogeneous nucleation follows a similar mechanism.

Higher levels of DOC were necessary to inhibit calcite precipitation when the  $P_{\text{CO}_2}$  increased at constant  $\Omega$ . Increase in the negative charge of the calcite crystals, decrease in the binding capacity of the DOC due to the decrease of the solution pH, and decrease in the DOC specific volume due to the increase in ionic strength may account for the lower inhibitory capability of DOC at higher  $P_{\text{CO}_2}$ .

The authors thank Christine Espiritu for her assistance in the chemical analysis. Contribution from the US Salinity Laboratory, USDA-ARS.

### REFERENCES

- Amankonah J. O. and Somasundaran P. (1985) Effects of dissolved mineral species on the electrokinetic behavior of calcite and apatite. *Coll. Surf.* **15**, 335–353.
- Back W. and Hanshaw B. B. (1970) Comparison of chemical hydrogeology of the carbonate peninsulas of Florida and Yucatan. *J. Hydrol.* **10**, 330–368.
- Barak P. and Chen Y. N. (1992) Equivalent radii of humic macromolecules from acid-base titration. *Soil Sci.* **154**, 184–195.
- Bartschat B. M., Cabaniss S. E., and Morel F. M. M. (1992) Oligoelectrolyte model for cation binding by humic substances. *Environ. Sci. Technol.* **26**, 284–294.
- Benedetti M. F., van Riemsdijk W. H., and Koopal L. K. (1996) Humic substances considered as a heterogeneous Donnan gel phase. *Environ. Sci. Technol.* **30**, 1805–1813.
- Brown C. A., Compton R. G., and Narramore C. A. (1993) The kinetics of calcite dissolution/precipitation. *J. Colloid Interface Sci.* **160**, 372–379.
- Buhmann D. and Dreybrodt W. (1985a) The kinetics of calcite dissolution and precipitation in geologically relevant situations of Karst areas. 1. Open-system. *Chem. Geol.* **48**, 189–211.
- Buhmann D. and Dreybrodt W. (1985b) The kinetics of calcite dissolution and precipitation in geologically relevant situations of Karst areas. 2. Closed-system. *Chem. Geol.* **53**, 109–124.
- Busenberg E. and Plummer L. N. (1986) A comparative study of the dissolution and crystal growth kinetics of calcite and aragonite. In *Studies in Diagenesis* (ed. F. A. Mumpton); *USGS Bull.* **1578**, 139–168.
- Charlet L., Wersin P., and Stumm W. (1990) Surface charge of  $\text{MnCO}_3$  and  $\text{FeCO}_3$ . *Geochim. Cosmochim. Acta* **54**, 2329–2336.
- Compton R. G. and Pritchard K. L. (1990) The dissolution of calcite at  $\text{pH} > 7$ : Kinetics and mechanism. *Phil. Trans. Royal Soc. London Ser. A Math. Phys. Sci.* **330**, 47–70.
- Compton R. G. and Unwin P. R. (1990) The dissolution of calcite in aqueous solution at  $\text{pH} < 4$ : Kinetics and mechanism. *Phil. Trans. Royal Soc. London Ser. A Math. Phys. Sci.* **330**, 1–46.
- Compton R. G., Pritchard K. L., and Unwin P. R. (1989) The dissolution of calcite in acid waters. Mass transport vs. surface control. *Freshwater Biol.* **22**, 285–288.
- Dandurand J. L., Gout R., Hoefs J., Menschel G., Schott J., and Usdowski E. (1982) Kinetically controlled variations of major components and carbon isotopes in a calcite-precipitating spring. *Chem. Geol.* **36**, 299–315.
- De Wit J. C. M., van Riemsdijk W. H., Nederlof L. K., Kinniburgh D. G., and Koopal L. K. (1990). Analysis of ion binding on humic substances and the determination of intrinsic affinity distributions. *Anal. Chim. Acta* **232**, 189–207.
- De Wit J. C. M., van Riemsdijk W. H., and Koopal L. K. (1993) Proton binding to humic substances. 1. Electrostatic effects. *Environ. Sci. Technol.* **27**, 2005–2014.
- Dove P. M. and Hochella M. F., Jr. (1993) Calcite precipitation mechanisms and inhibition by orthophosphate: In situ observations by scanning force microscopy. *Geochim. Cosmochim. Acta* **57**, 705–714.
- Dreybrodt W. (1981) The kinetics of calcite precipitation from thin films of calcareous solutions and the growth of speleothems: Revisited. *Chem. Geol.* **32**, 237–245.
- Engelbreton R. R., Amos T., and von Wandruszka R. (1996) Quantitative approach to humic acid associations. *Environ. Sci. Technol.* **30**, 990–997.
- Gratz A. J. and Hillner P. E. (1993) Poisoning of calcite growth viewed in the atomic force microscope (AFM). *J. Cryst. Growth* **129**, 789–793.
- Inskip W. P. and Bloom P. R. (1985) An evaluation of rate equations for calcite precipitation kinetics at  $P_{\text{CO}_2}$  less than  $0.01 \text{ atm}$  and  $\text{pH}$  greater than 8. *Geochim. Cosmochim. Acta* **49**, 2165–2180.
- Inskip W. P. and Bloom P. R. (1986) Kinetics of calcite precipitation in the presence of water soluble organic ligands. *Soil Sci. Soc. Amer. J.* **50**, 1167–1172.
- Jacobson R. L. and Usdowski E. (1975) Geochemical controls on a calcite precipitating spring. *Contrib. Mineral. Petrol.* **51**, 65–74.
- Katz J. L., Reick M. R., Herzog E. R., and Parsiegla K. I. (1993) Calcite growth inhibition by iron. *Langmuir* **9**, 1423–1430.
- Kinniburgh D. G. (1986) General purpose adsorption isotherms. *Environ. Sci. Technol.* **20**, 895–904.
- Kitano Y. and Hood D. W. (1965) The influence of organic material on the polymorphic crystallization of calcium carbonate. *Geochim. Cosmochim. Acta* **29**, 29–41.
- Last W. M. (1982) Holocene carbonate sedimentation in Lake Manitoba, Canada. *Sedimentol.* **29**, 691–704.
- Lebron I. and Suarez D. L. (1996) Calcite nucleation and precipitation kinetics as affected by dissolved organic matter at  $25^\circ\text{C}$  and  $\text{pH} > 7.5$ . *Geochim. Cosmochim. Acta* **60**, 2765–2776.
- Lorah M. M. and Herman J. S. (1988) The chemical evolution of a travertine-depositing stream: Geochemical processes and mass transfer reaction. *Water Resour. Res.* **24**, 1541–1552.
- Marinsky J. A. and Ephraim J. (1986) A unified physicochemical description of the protonation and metal ion complexation equilibria of natural organic acids (humic and fulvic acids). 1. Analysis of the influence of polyelectrolyte properties on protonation equilibria in ionic media: fundamental concepts. *Environ. Sci. Technol.* **20**, 349–354.
- Milne C. J., Kinniburgh D. G., De Wit J. C. M., van Riemsdijk W. H., and Koopal L. K. (1995) Analysis of proton binding by a peat humic

- acid using a simple electrostatic model. *Geochim. Cosmochim. Acta* **59**, 1101–1112.
- Mishra S. K. (1978) The electrokinetics of apatite and calcite in inorganic electrolyte environment. *Intl. J. Mineral Proc.* **5**, 69–83.
- Morse J. W. (1983) The kinetics of calcium carbonate dissolution and precipitation. In *Carbonates: Mineralogy and Chemistry* (ed. R. J. Reeder); *Rev. Mineral.* **11**, 227–264.
- Mucci A. (1986) Growth kinetics and composition of magnesian calcite overgrowths precipitated from seawater: Quantitative influence of orthophosphate ions. *Geochim. Cosmochim. Acta* **50**, 2255–2265.
- Mucci A. and Morse J. W. (1983) The incorporation of  $Mg^{2+}$  and  $Str^{2+}$  into calcite overgrowths: Influences of growth rate and solution composition. *Geochim. Cosmochim. Acta* **47**, 217–233.
- Murphy E. M. and Zachara J. M. (1995) The role of sorbed humic substances on the distribution of organic and inorganic contaminants in groundwater. *Geoderma* **67**, 103–124.
- Nancollas G. H. and Reddy M. M. (1971) The crystallization of calcium carbonate II. Calcite growth mechanism. *J. Colloid Interface Sci.* **10**, 215–252.
- Nielsen A. E. (1983) Precipitates: Formation, coprecipitation, and aging. In *Treatise on Analytical Chemistry* (ed. I. M. Kolthoff and P. J. Elving), pp. 269–347. Wiley.
- Paquette J., Vali H., and Mucci A. (1996) TEM study of Pt-C replicas of calcite overgrowths precipitated from electrolyte solutions. *Geochim. Cosmochim. Acta* **60**, 4689–4699.
- Parker D. R., Norvell W. A., and Chaney R. L. (1994) GEOCHEM-PC: A chemical speciation program for IBM and compatible personal computers. In *Soil Chemical Equilibrium and Reaction Models* (ed. R. H. Loeppert et al.); *SSSA Spec. Publ.* **42**, 253–270.
- Plummer L. N., Wigley T. M. L., and Parkhurst D. L. (1978) The kinetics of calcite dissolution in  $CO_2$ : Water systems at 5–60°C and 0.0–1.0 atm  $CO_2$ . *Amer. J. Sci.* **278**, 179–216.
- Plummer L. N., Wigley T. M. L., and Parkhurst D. L. (1979) Critical review of the kinetics of calcite dissolution and precipitation. In *Chemical Modeling in Aqueous Systems* (ed. E. A. Jenne); *Amer. Chem. Soc. Symp. Ser.* **93**, 537–573.
- Reddy M. M. (1977) Crystallization of calcium carbonate in the presence of trace concentrations of phosphorous containing anions. I. Inhibition by phosphate and glycerophosphate ions at pH 8.8 and 25°C. *J. Cryst. Growth* **41**, 287–295.
- Reddy M. M. and Nancollas G. H. (1973) Calcite crystal growth inhibition by phosphonates. *Desalination* **12**, 61–73.
- Reddy M. M. and Wang K. K. (1980) Crystallization of calcium carbonate in the presence of metal ions. I. Inhibition by magnesium ion at pH 8.8 and 25°C. *J. Cryst. Growth* **50**, 470–480.
- Reddy M. M., Plummer L. N., and Busenberg E. (1981) Crystal growth of calcite from calcium bicarbonate solutions at constant  $P_{CO_2}$  and 25°C: A test of a calcite dissolution model. *Geochim. Cosmochim. Acta* **45**, 1281–1289.
- Reynolds R. C., Jr. (1978) Polyphenol inhibition of calcite precipitation in Lake Powell. *Limnol. Oceanogr.* **23**, 585–597.
- Shiraki R. and Brantley S. (1995) Kinetics of near-equilibrium calcite precipitation at 100°C: An evaluation of elementary reaction-based and affinity-based rate laws. *Geochim. Cosmochim. Acta* **59**, 1457–1471.
- Somasundaran P. and Agar G. E. (1967) The zero point of charge of calcite. *J. Colloid Interface Sci.* **24**, 433–440.
- Sposito G., Holtzclaw K. M., and Baham J. (1976) Analytical properties of the soluble, metal-complexing fractions in sludge-soil mixtures: II. Comparative structural chemistry of fulvic acid. *Soil Sci. Soc. Amer. J.* **40**, 691–697.
- Suarez D. L. (1977) Ion activity products of calcium carbonate in waters below the root zone. *Soil Sci. Soc. Amer. J.* **41**, 310–315.
- Suarez D. L. (1983) Calcite supersaturation and precipitation kinetics in the lower Colorado River, All-American Canal, and East Highline Canal. *Water Resour. Res.* **19**, 653–661.
- Suarez D. L. and Rhoades J. D. (1982) The apparent solubility of calcium carbonate in soils. *Soil Sci. Soc. Amer. J.* **46**, 716–722.
- Suarez D. L., Wood J. D., and Ibrahim I. (1992) Reevaluation of calcite supersaturation in soils. *Soil Sci. Soc. Amer. J.* **56**, 1776–1784.
- Thompson D. W. and Pownall P. G. (1989) Surface electrical properties of calcite. *J. Colloid Interf. Sci.* **131**, 74–83.
- Tipping E. and Hurley M. A. (1992) A unifying model of cation binding by humic substances. *Geochim. Cosmochim. Acta* **56**, 3627–3641.
- Van Cappellen P., Charlet L., Stumm W., and Wersin P. (1993) A surface complexation model of the carbonate mineral-aqueous solution interface. *Geochim. Cosmochim. Acta* **57**, 3505–3518. [j102]